

A quinoline based pH sensitive ratiometric fluorescent sensor: Structure and spectroscopy

SOMA MUKHERJEE^{a,*}, AMIT KUMAR PAUL^a and HELEN STOECKLI-EVANS^b

^aDepartment of Environmental Science, University of Kalyani, Kalyani, Nadia 741 235, West Bengal, India

^bInstitute of Physics, University de Neuchatel, CH–2000 Neuchatel, Switzerland

e-mail: sommukh445@yahoo.co.in; somam580@gmail.com

MS received 2 April 2015; revised 23 June 2015; accepted 25 June 2015

Abstract. A new quinoline based hydrazone was synthesized via a condensation reaction and characterized by NMR, mass and single crystal X-ray diffraction studies. It was investigated for suitability as a reversible ratiometric fluorescent pH sensor in acidic pH region. The sensor exhibits intramolecular charge transfer (ICT) type photophysical changes upon protonation of the quinoline ring. No significant interference on emission behavior was observed in the presence of various metal ions.

Keywords. ICT; Ratiometric; Fluorescent pH sensor; Quinoline hydrazone; Structure.

1. Introduction

Analytic estimation of ion concentration through rationally designed molecular receptors is an active field of research. Various photophysical properties can be exploited for selective detection of an analyte. Fluorescence sensors are powerful tools for sensing biologically and environmentally important ions due to its superior selectivity, sensitivity and non-invasive approach.^{1–3} Among other fluorescence phenomenon that is being utilized for sensing purpose, intramolecular charge transfer (ICT) process has some distinctive advantages.^{4,5} It is generally accompanied by significant emission wavelength shift or Stokes shift upon interaction with the analyte permitting ratiometric estimation. pH is a vital parameter for biological systems⁶ as it controls enzymatic activity, cell proliferation, apoptosis, etc. Fluorescence pH sensors are emerging as crucial tools for visualizing noninvasive intracellular pH distribution.^{7–11} Besides this, fluorescent pH sensors are also applicable for imaging pH gradient in biofilms¹² providing important information about its microenvironment. In this work, we have synthesized and characterized a quinoline based fluorescent probe^{13–16} as a new ratiometric fluorescent pH sensor. The sensor displayed high sensitivity over the acidic pH range (3.5–5.5) and no significant interference was observed in the presence of various metal ions.

2. Experimental

2.1 Materials and general methods

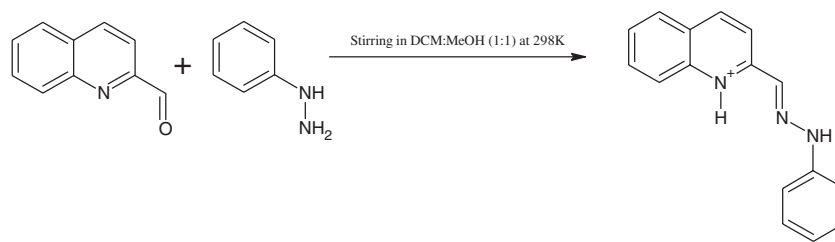
All analytic grade reagents were purchased commercially. FTIR data were collected with the help of Spectrum One FT-IR Spectrometer. NMR spectra were recorded on a Bruker DRX-400 spectrometer with TMS as the internal standard in DMSO-*d*₆. Absorption spectra were measured on a Shimadzu UV-1700 spectrophotometer. Fluorescence measurements were performed on a Hitachi F7000 spectrofluorimeter. Mass spectra measurement was carried out by Waters Xevo G2-S QToF Mass Spectrometer. pH measurements were carried out using Orion 3-Star Plus pH Benchtop Meter.

2.2 Synthesis

The compound **1** was synthesized by stirring an equimolar amount of quinoline-2-aldehyde (0.2 m M, 0.031 g) and *p*-tolyl hydrazine (0.2 mM, 0.024 g) in methanol-dichloromethane (1:1 v/v) at room temperature for 30 min. The desired product was obtained in good yield by slow evaporation of this solution.^{8,17} The deprotonated form of **1** was prepared by adding few drops of methanolic 1N KOH to the solution of **1** (scheme 1).

1: Yield: 0.044 g (82%). C₁₇H₁₅N₃, ¹H NMR 10.9 (1, s), 8.29 (1, s), 8.13–8.11 (1, d), 8.00–7.95 (3, m), 7.93 (1, t), 7.73 (1, s), 7.57–7.55 (1, m), 7.10 (4, s), 2.24 (3, s); m/z (ESI) [M+H]⁺ 262.1(calculated 262.3). FTIR (KBr pellet, cm⁻¹): 3384, 2915, 1639, 1601, 1547,

*For correspondence



Scheme 1. Synthesis.

1499, 1410, 1385, 1346, 1295, 1268, 1234, 1195, 1148, 1123, 1060, 768, 616.

2.3 X-ray crystallography

The compound **1** was crystallized in the protonated form by slow evaporation of a methanolic solution. The intensity data were collected at 173 K on a Stoe Mark II-Image Plate Diffraction System¹⁸ equipped with a two-circle goniometer and using MoK α graphite monochromated radiation ($\lambda = 0.71073 \text{ \AA}$). The structure was solved by direct methods with SHELXS-97.¹⁹ The refinement and all further calculations were carried out with SHELXL-97.¹⁹ The NH and water H-atoms were located in difference Fourier maps and freely refined. The C-bound H-atoms were included in calculated positions and treated as riding atoms: C-H = 0.95–0.98 \AA with $U_{\text{iso}}(\text{H}) = 1.5U_{\text{eq}}$ (parent C-atom) for methyl H atoms and 1.2 U_{eq} (parent C-atom) for other H atoms. The non-H atoms were refined anisotropically, using weighted full-matrix least-squares on F^2 . A semi-empirical (multi-scan) absorption correction was applied using the MULABS routine in PLATON.²⁰ The molecular structure with the crystallographic numbering scheme, together with the crystal packing are

illustrated in figures 1–3, drawn using the program Mercury.²¹ Further crystallographic data and refinement details are given in table 1.

2.4 Sample preparation for UV-Vis and fluorescence measurements

A stock solution of **1** (0.5 mM) was prepared in MeOH. The solutions for spectroscopic measurements were obtained by diluting the stock solutions to 5 mL ($1 \times 10^{-5} \text{ M}$) by deionized water. In the titration experiment, 3 mL solution of **1** ($1 \times 10^{-5} \text{ M}$) was poured into a quartz optical cell of 1 cm path length each time and slight pH variations of the solution were achieved by adding minimum volume of NaOH or HCl. The pH of the solution was measured for each measurement. The fluorescence titration experiment was investigated in a similar procedure with ($5 \times 10^{-5} \text{ M}$) solution and the excitation wavelength was 310 nm. Quantum yields (Q) were calculated in aqueous medium ($\text{CH}_3\text{CN}/\text{H}_2\text{O}$ (1:4, v/v) solvent system) by secondary method with respect to the quinine sulfate ($\Phi = 0.55$ in 0.1 M H_2SO_4) as standard,²² using eq. (1):

$$Q = Q_R \times (I/I_R) \times (OD_R/OD) \times \eta^2/\eta_R^2 \quad (1)$$

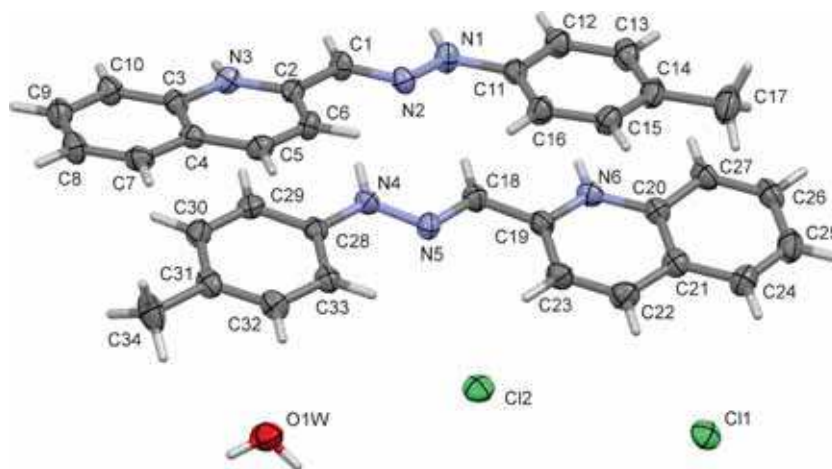


Figure 1. A view of the molecular structure of compound **1** with atom labelling. Displacement ellipsoids are drawn at the 50% probability level.

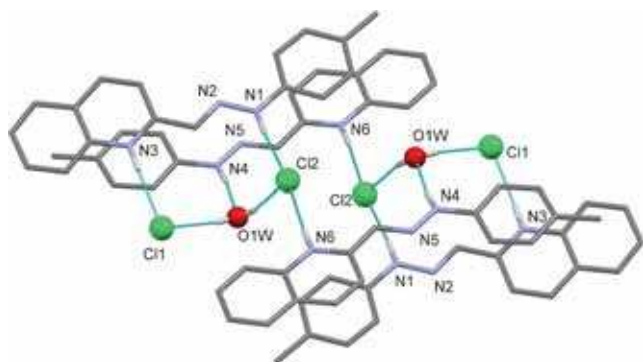


Figure 2. A view of the hydrogen bonded tetramer-like unit, possessing inversion symmetry. Hydrogen bonds are shown as sky blue colored dotted line.

where, Q is the quantum yield, I is the integrated area corresponding to the fluorescence spectrum, OD is the optical density, and η is the refractive index. The subscript R refers to the reference fluorophore of known quantum yield.

To determine the fluorescence response of **1** to different metal cations, the stock solution of **1** was diluted to 1×10^{-5} M with phosphoric acid buffer (pH 7.4) and acetic acid- sodium acetate buffer (pH 4.0) for interference study at the working pH range. The interference was measured by adding metal salt solutions and measuring the emission after complete mixing.

3. Results and Discussion

3.1 Synthesis

The compound **1** was synthesized following a general procedure.^{8,17} It was characterized by ^1H NMR, mass and single crystal X-ray diffraction studies (scheme 2).

3.2 Single crystal X-ray diffraction studies

The molecular structure of compound **1** was confirmed by single crystal X-ray diffraction studies. It crystallized in the protonated form with two independent cations (A involving atoms N1-N3, and B involving atoms N4-N6, two Cl^- anions and a water molecule of crystallization in the asymmetric unit (figure 1). Both cations (A and B) are essentially planar with the benzene ring being inclined to the mean plane of the protonated quinoline moiety by $6.46(14)^\circ$ in cation A and $3.24(14)^\circ$ in cation B. The bridging C11-N1-N2-C1 and C28-N4-N5-C18 torsion angles are $-179.6(3)$ and $-178.0(3)^\circ$, respectively.

In the crystal of **1**, the cations, anions and the water molecule and linked by N-H...O, N-H...Cl and O-H...Cl hydrogen bonds (table S1 in Supplementary Information) forming a tetramer-like unit possessing inversion symmetry (figure 2). These units in turn are linked by C-H...Cl and C-H...O hydrogen bonds and

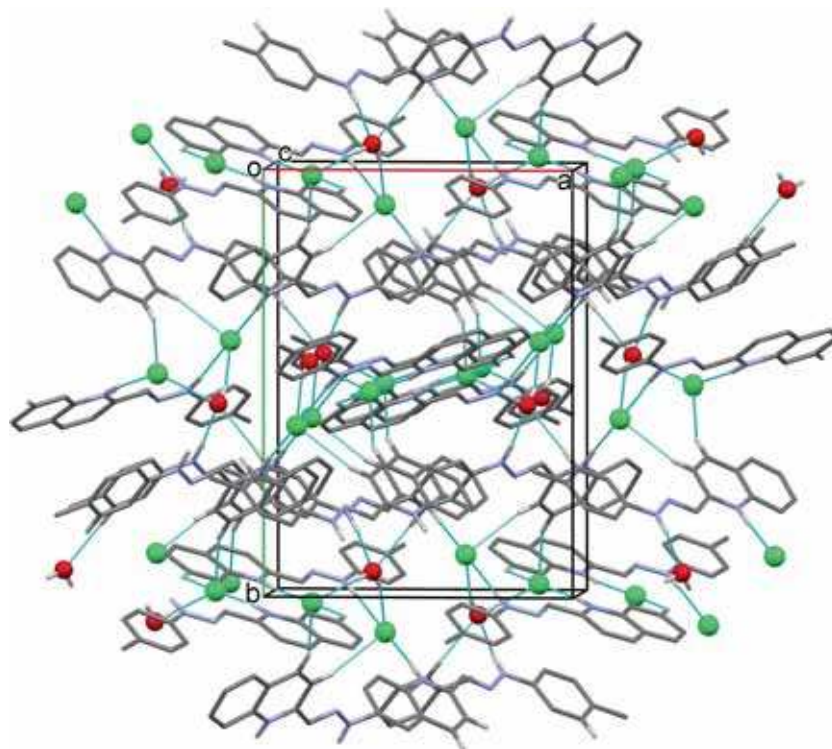


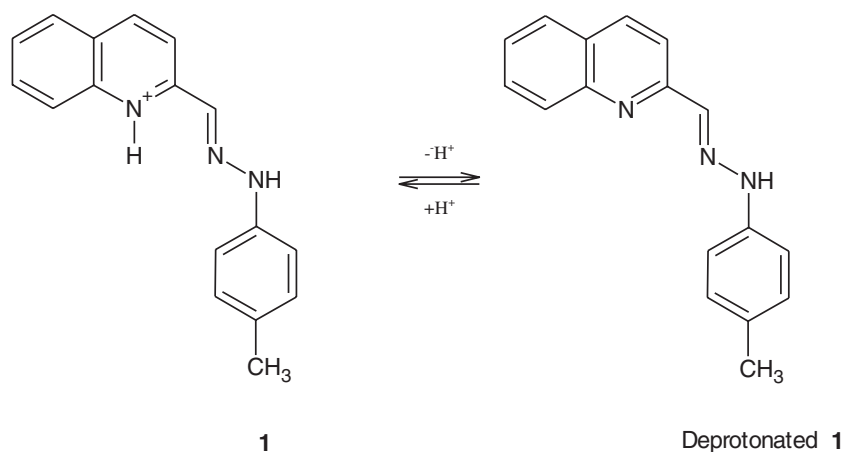
Figure 3. A view along the c axis of the crystal packing of compound **1**. Hydrogen bonds are shown as dashed lines.

Table 1. Crystallographic data and structure refinement parameters for **1**.

	1
Formula	$[\text{C}_{17}\text{H}_{16}\text{N}_3]^+\text{Cl}^- \cdot 0.5(\text{H}_2\text{O})$
M_r (g mol ⁻¹)	306.79
Cryst. dimension (mm)	0.45, 0.35, 0.19
Space group	P 2 ₁ /a
T (K)	173(2)
a (Å)	13.007(1)
b (Å)	17.3207(9)
c (Å)	14.7900(11)
α (°)	90.00
β (°)	103.129(6)
γ (°)	90.00
V (Å ³)	3244.9(4)
Z	8
D_{calc} (g/cm ³)	1.256
μ (mm ⁻¹)	0.236
$F(000)$	1288
θ Range (°)	1.41–25.69
Reflections measured	24754
Reflections unique	6115
R (int)	0.127
Reflections observed [$I > 2s(I)$]	3478
Data/parameters	6115/408
GOF	1.005
^a R_1 , wR_2^b [$I > 2\sigma(I)$]	0.0739, 0.1017
^b R_1 , wR_2^b (all data)	0.1402, 0.1171
Largest diff peak and hole [eÅ ⁻³]	0.198, -0.237

^a $R_1 = [\sum||F_o - |F_c||]/\sum|F_o|$ (based on F)

^b $wR_2 = [[\sum w(|F_o^2 - F_c^2|)^2]/[\sum w(F_o^2)^2]]^{1/2}$ (based on F^2)

**Scheme 2.** Protonated and deprotonated forms of **1**.

C-H... π (table S1) and $\pi - \pi$ interactions [centroid-to-centroid distances vary from 3.684(2) to 3.784(2) Å] forming a three-dimensional framework structure (figure 3).

3.3 Spectroscopic responses to pH

In aqueous medium (1% methanol, pH 7.0) the compound **1** exhibits a strong absorption band at 374 nm

which gradually decreases with decreasing pH up to 2.0 followed by the generation of a new peak centered at 455 nm (figure 4). Further decrease in pH does not induce any change in the spectrum. Increasing pH of the same solution exhibits similar spectral pattern indicating that the changes are completely reversible. This spectral change was also detected optically as the color of the solution changes from red to faint yellow as the pH of the medium increases.

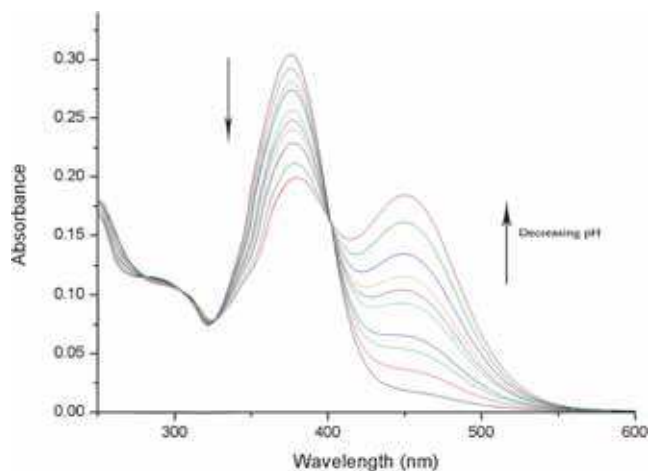


Figure 4. Absorption spectra of **1** (1.0×10^{-5} M) in aqueous solution (1% methanol) at different pH (7.0, 6.5, 6.0, 5.75, 5.25, 4.75, 4.25, 3.75, 3.25, 2.75).

In aqueous solution (pH = 7.0, 1% methanol) **1** emits at 455 nm ($\lambda_{\text{ex}} = 310$ nm, an isosbestic point) with a large Stokes shift of 81 nm. With the gradual decrease of pH from 7.0 to 2.75 the emission band undergoes a significant red shift to 507 nm. The pK_a values of **1** were found to be 4.84 (absorbance) and 4.76 (fluorescence), respectively, as calculated from Henderson - Hasselbalch equation, ($\text{pH} = \text{pK}_a + \log([\text{salt}]/[\text{acid}])$) (figures 5 and 6). This photophysical change due to the lowering of pH of the medium can be attributed to the protonation of the quinoline ring which in turn promotes stronger charge transfer from the benzene ring.^{8,23} To get an insight into the solvatochromic behavior of the protonated and deprotonated forms, the spectral dependency of **1** on solvent polarity was examined. It was found that both the absorption and emission spectra of **1** and deprotonated **1** show bathochromic shifts with increasing solvent polarity (table 2) which might be due

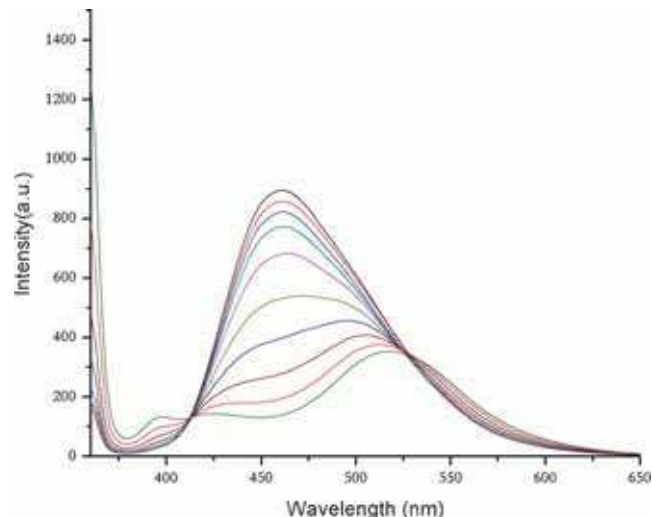


Figure 6. Emission spectra of **1** (5.0×10^{-5} M) at different pH (7.0, 6.5, 6.0, 5.75, 5.25, 4.75, 4.25, 3.75, 3.25, 2.75). $\lambda_{\text{ex}} = 310$ nm.

the internal charge transfer. A plot of intensity ratio, I_{455}/I_{507} against pH for **1** is shown in figure 7. The quantum yield for the compound **1** in pH 7 was determined as 0.009. The reversible nature and reproducibility of the sensor was tested by recording the ratio of fluorescence intensity at 507 nm and 445 nm with the change of pH in 4 to 7 range, and vice versa, up to 6 cycles (figure 8). Thus, the sensor might be applicable for real time pH monitoring.

To establish its applicability in biological systems where different metal ions are present in cellular or extracellular environment, selectivity of **1** towards different metal ions such as Na^+ , K^+ , Ca^{2+} , Mg^{2+} , Cu^{2+} , Ni^{2+} , Mn^{2+} , Fe^{2+} , Zn^{2+} and Fe^{3+} in aqueous solution (1% methanol) emission spectra were recorded at pH 7.4 and 4.0. No obvious change in the emission

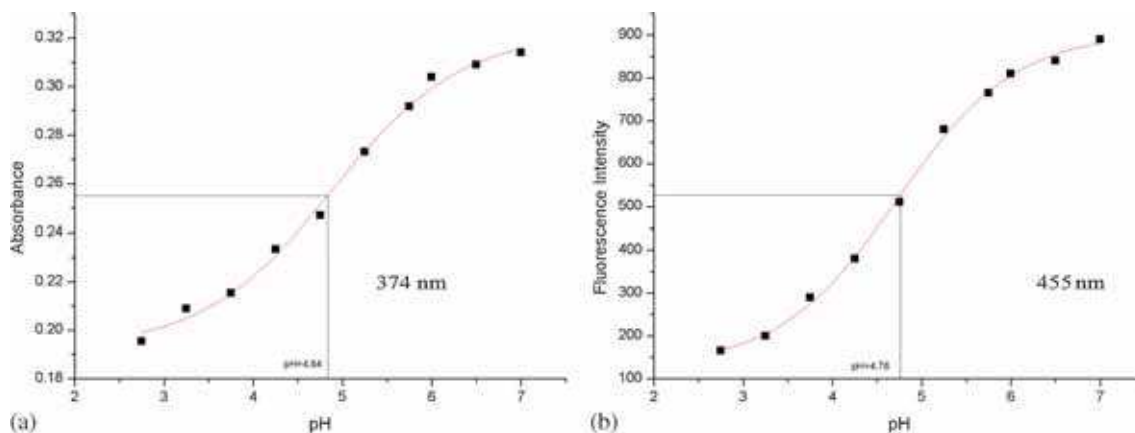
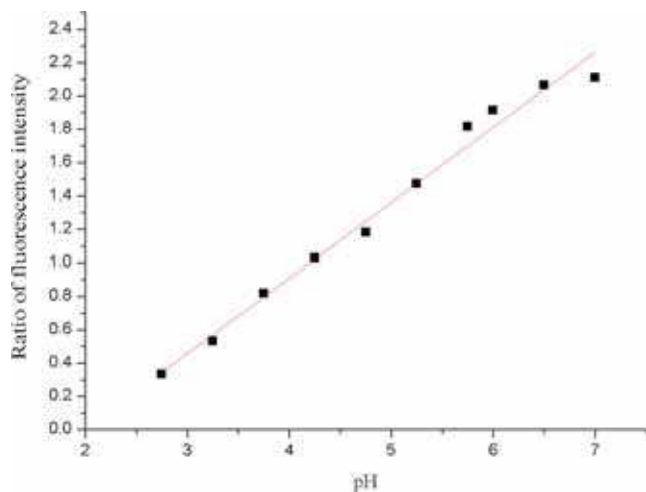
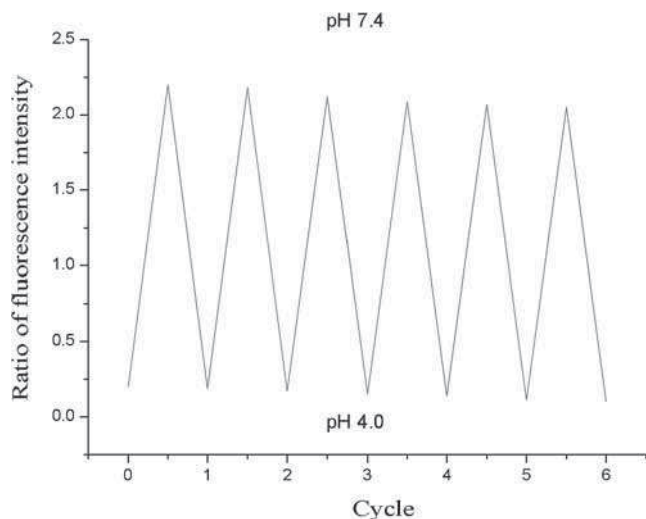


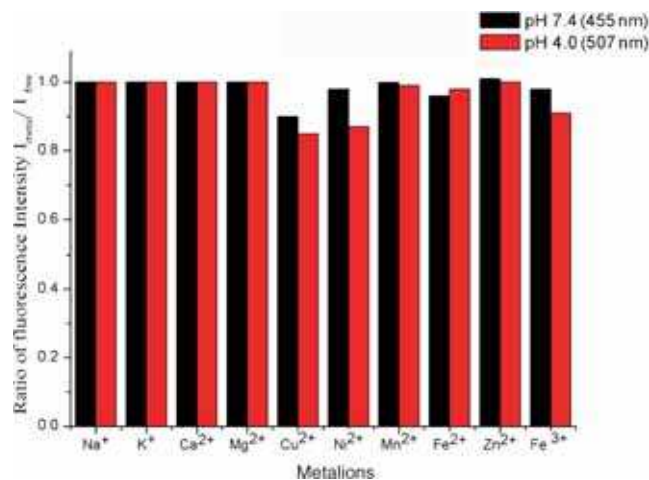
Figure 5. (a) Plot of absorbance of **1** at 374 nm and; (b) Plot of fluorescence intensity at 455 nm as a function of pH.

Table 2. Solvent dependent absorption and emission maxima (in nm) of **1**.

Solvent	deprotonated 1		1	
	λ_{abs}	λ_{fl}	λ_{abs}	λ_{fl}
DMSO	378	445	448	501
MEOH	376	442	442	495
DCM	374	435	441	482
CHCl ₃	370	431	437	480

**Figure 7.** Ratiometric curve of I_{455}/I_{507} as a function of pH.**Figure 8.** The ratio of fluorescence intensity at 455 nm and 507 nm of **1** ($\lambda_{\text{ex}} = 310$ nm, 5.0×10^{-5} M in 1% aqueous methanol) upon consecutive addition of 1(N) HCl and 1(N) NaOH solution up to 6 cycles.

ratio was observed, even though manifold equivalents of metal ions were added to **1** (figure 9).

**Figure 9.** Ratio of fluorescence intensity of **1** (5.0×10^{-5} M, $\lambda_{\text{ex}} = 310$ nm) at 455 nm (pH 7.4) and 507 nm (pH 4.0) in aqueous solution (1% methanol) in the presence of various metal ions, at ratio 10:1 (other ions: **1**) for Cu^{2+} , Ni^{2+} , Mn^{2+} , Fe^{2+} , Zn^{2+} and Fe^{3+} , while for Na^+ , K^+ , Ca^{2+} and Mg^{2+} , the ratio is $10^5:1$.

4. Conclusion

In summary, we have synthesized and characterized an ICT based ratiometric fluorescent pH sensor with large Stokes shift through condensation of quinoline aldehyde and *p*-tolyl hydrazine. The molecular structure of this hydrazone was determined by single crystal X-ray diffraction studies. The sensor exhibits reversible absorption and emission change in the acidic region and the consequent photophysical change can easily be detected by naked eye and ratiometric measurements.

Supplementary Information

CCDC 1055117 contains the supplementary crystallographic data for compound **1**. These data can be obtained free of charge via <http://www.ccdc.cam.ac.uk/conts/retrieving.html>, or from the Cambridge Crystallographic Data Centre, 12 Union Road, Cambridge CB2 1EZ, UK; fax: (+44) 1223-336-033; or e-mail: deposit@ccdc.cam.ac.uk. Details of the hydrogen bond

geometry (table S1) are available at www.ias.ac.in/chemsci.

Acknowledgements

Financial support received from DST-FIST and DST-PURSE, New Delhi and the Indo-Swiss Joint Research Programme (ISJRP) for Joint Utilization of Advanced Facilities (JUAF) are gratefully acknowledged. We are thankful to the University of Kalyani for providing infrastructural facilities.

References

1. Yang Y, Zhao Q, Feng W and Li F 2013 *Chem. Rev.* **113** 192
2. Schäferling M 2012 *Angew. Chem. Int. Ed.* **51** 3532
3. Wu J, Liu W, Ge J, Zhang H and Wang P 2011 *Chem. Soc. Rev.* **40** 3483
4. Yu F, Li P, Song P, Wang B, Zhao J and Han K 2012 *Chem. Commun.* **48** 2852
5. Mei Y and Bentley P A 2006 *Bioorg. Med. Chem. Lett.* **16** 3131
6. Roos A and Boron W F 1981 *Physiol. Rev.* **61** 296
7. Wang R, Yu C, Yu F, Chen L and Yu C 2010 *TrAC Trends Anal. Chem.* **29** 1004
8. Mukherjee S, Paul A K, Rajak K K and Stoeckli-Evans H 2014 *Sens. Actuators B: Chem.* **203** 150
9. Han J and Burgess K 2010 *Chem. Rev.* **110** 2709
10. Briggs M S, Burns D D, Cooper M E and Gregory S J 2000 *Chem. Commun.* 2323
11. Saha U C, Dhara K, Chattopadhyay B, Mandal S K, Mondal S, Sen S, Mukherjee M, Smaalen S V and Chattopadhyay P 2011 *Org. Lett.* **13** 4510
12. Schlafer S, Garcia J E, Greve M, Raarup M K, Nyvad B and Dige I 2015 *Appl. Environ. Microbiol.* **81** 1267
13. Kalogianni A, Pefkianakis E, Stefopoulos A, Bokias G and Kallitsis J K 2010 *J. Polym. Sci. Polym. Phys.* **48** 2078
14. Moutsiopoulou A, Andreopoulou A K, Lainioti G, Bokias G, Voyiatzis G and Kallitsis J K 2015 *Sens. Actuators B: Chem.* **211** 235
15. Zhu S, Lin W and Yuan L 2013 *Dyes Pigm.* **99** 465
16. Phukan S, Saha M, Pal A K and Mitra S 2013 *J. Mol. Struct.* **1039** 119
17. Mukherjee S, Paul A K and Stoeckli-Evans H 2014 *Sens. Actuators B: Chem.* **202** 1190
18. Stoe & Cie 2009 X-Area & X-RED32. Stoe & Cie GmbH, Darmstadt, Germany
19. Sheldrick G M 2008 *Acta Cryst. A* **64** 112
20. Spek A L 2009 *Acta Cryst. D* **65** 148
21. Macrae C F, Bruno I J, Chisholm J A, Edgington P R, McCabe P, Pidcock E, Rodriguez-Monge L, Taylor R, van de Streek J and Wood P A 2008 *J. App. Cryst.* **41** 466
22. Fletcher A N 1969 *Photochem. Photobiol.* **9** 439
23. Niu W, Fan L, Nan M, Li Z, Lu D, Wong M S, Shuang S and Dong C 2015 *Anal. Chem.* **87** 2788